Evaluation of Reactive Power Control Capabilities of Residential PV in an Unbalanced Distribution Feeder

John Seuss[1], Matthew J. Reno[1,2], Robert J. Broderick[2], Ronald G. Harley[1]

[1]Georgia Institute of Technology, Atlanta, GA, USA
[2]Sandia National Laboratories, Albuquerque, NM, USA

***Abstract* — The use of residential PV grid-tie inverters to supply reactive power as a benefit to the distribution grid has been widely proposed, however, there is little insight into how much of a benefit can be achieved from this control under varying system operating points. This paper seeks to demonstrate the effectiveness of a linearized versus nonlinear reactive power dispatch solution on a highly unbalanced distribution feeder under differing load profiles, insolation levels, and penetration rates of PV in the feeder. The results are analyzed to determine the system operating points that are favorable to reactive power control and the overall effectiveness of each solution in realistic feeder states.**

***Index Terms* — photovoltaic systems, reactive power control, voltage control, particle swarm optimization.**

I. Introduction

Photovoltaic (PV) energy generation continues to be one of the fastest growing sectors of the energy mix. Residential rooftop PV is a particularly fast growing sector and many medium voltage residential distribution networks already have over 25% penetration of PV generators [1][2]. This rapid growth is outpacing utility interconnection standards, which still consider the small rooftop PV units to be of insignificant size, but collectively the PV are beginning to pose a number of stability and power quality problems in low- and medium-voltage distribution networks [3][4]. One potential solution to mitigate the problems caused by abundant PV is to use the spare reactive power capacity of their grid-tie inverters collectively to benefit the distribution network as a whole.

Current interconnection standards do not allow for dynamic reactive power control of small-scale distributed PV, however, there are indications that this standard may change soon and indeed many new inverters are being manufactured with the capability to adjust their power factor via a remote signal [5][6]. In fact, many reactive power control strategies have been proposed for distributed generation in distribution networks recently. There is a large focus on using local voltage measurements and coordinated local droop controls to provide reactive power support, similar to how generators share power deviations [7-9]. The benefit of this method is there is no need for a communication network. However, many modern distribution networks have communication networks to support other smart grid functions, which some research has proposed to repurpose to dispatch reactive power in a centralized fashion [10]. Other research propose hybrid or distributed approaches that take advantage of local communications to work around the scalability probable of centralized control in large networks [11].

However, it is not certain from many of these papers how much the reactive power control will actually benefit the distribution network under varying conditions. The goal of this research is to quantify the benefit of the reactive power capabilities of the PV systems from a system-level viewpoint on any given network under different loading and insolation conditions. Since this goal requires solving a complex optimization problem many times, a linear approximation is developed in order to quickly reach a dispatch solution for any given network operating point. A comparison between a fully nonlinear optimization solution and the linearized approximate solution is made for a given daily load and insolation profile on the IEEE 13-bus feeder.

This paper is organized as follows. Section II will develop the optimum reactive power dispatch problem that is to be considered. Section III will develop the solution methods for the optimization problem from Section II. Section IV will present and analyze the simulation results and Section V will provide future directions and conclusions.

II. Optimum Reactive Power Dispatch Problem

There are many different objectives that can be achieved by reactive power injection [7]. This research focuses on the objectives of voltage deviation from nominal and line loss minimization. These goals are the most desirable to utilities facing high PV penetration and the most easily met with reactive power support [3]. Each inverter is assumed to be dispatched from a centralized control with full knowledge of the distribution network. This allows for a best-case-scenario for the inverter resources that are available at a given system operating point. Inverter dynamics are assumed to be much faster than the time scale being analyzed, so only steady-state inverter operating points need to be found for each system operating point. The real power output of the inverters is assumed to track the maximum power point of the PV panels based on the amount of insolation and the inverter rating as follows:

$$p_i^g(t) = S_i^{rated} I(t) \tag{1}$$

$$q_i^{g,max}(t) = \sqrt{(S_i^{rated})^2 - \left(p_i^g(t)\right)^2} = S_i^{rated}\sqrt{1 - I(t)^2} \tag{2}$$

Under the assumption of "watt priority" control, the real power output, p_i^g, is a proportion of the inverter rating, S_i^{rated}, based on the insolation $I \in [0,1]$ and the reactive power output, q_i^g, is constrained by the remaining inverter capacity available at each insolation level. Inverter overrating, high DC to AC plant design ratios, and power factor limits are not considered in this paper, but could be easily added.

At each network operating point, the state of the system consisting of the distribution network and the controllable inverters can be described by the complex voltages of each network node, or $\boldsymbol{x} = [\boldsymbol{V}\ \boldsymbol{\theta}]^T$, which are determined by the solution of the power flow equations, $\boldsymbol{G}(\boldsymbol{x}, \boldsymbol{u}, \boldsymbol{d})$, with the controllable inputs to the system being the reactive power output of the inverters, $\boldsymbol{u} = \boldsymbol{q^g}$ and $\boldsymbol{d} = [\boldsymbol{p^c}\ \boldsymbol{q^c}\ \boldsymbol{p^g}]^T$ being the particular state of the system load (real and reactive power consumption) and PV real power output (1). Using these definitions, the problem of optimizing reactive power injection to minimize a deviation from the nominal line voltage, V^*, and total line losses can be described by

$$\begin{aligned} \min_{\boldsymbol{u}} J(\boldsymbol{x}, \boldsymbol{u}) &= w_1 \sum_{i=1}^{n} (V_i - V^*)^2 + w_2 \sum_{j=1}^{m} L_j \\ s.t. \quad & \boldsymbol{G}(\boldsymbol{x}, \boldsymbol{u}, \boldsymbol{d}) = \boldsymbol{0} \\ & |u_i| \le q_i^{g,max}(t) \end{aligned} \tag{3}$$

Simply put, J scores how well a potential solution, $\boldsymbol{u}$, achieves the goals of minimizing feeder line voltage deviation from the nominal value and total line losses, L, while not exceeding the available reactive power of each PV inverter (2). The relative importance of one goal over the other can be adjusted by the weights w_1, w_2. Although the nonlinear system equations, $\boldsymbol{G}(\boldsymbol{x}, \boldsymbol{u}, \boldsymbol{d})$, have been shown to have a unique solution under normal operating conditions [12], the solutions that minimize (3) are not guaranteed to be unique. For instance, considering only the voltage regulation problem, if a system with n buses has p controllable inverters at separate buses of sufficient size to regulate the voltage of their bus equally on either side of the desired nominal voltage may achieve two solutions that satisfy (3). This situation is depicted in Fig. 1 where the two nodes depicted with stars have reactive power generation and the node between them does not. Two possible solutions that equally minimize voltage deviation are evident.

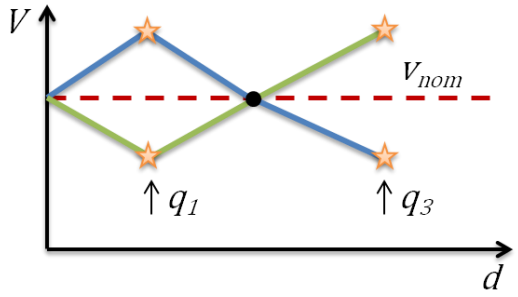

Fig 1. Two possible feeder voltage profiles that satisfy (3) based on reactive power injections q_1 and q_3 at some distance, d, down the

By this logic, for an entire feeder, there exist at least 2^{n-p} "optimum" solutions, which is not ideal for numerical methods that may have trouble converging on a minima. This emphasizes the need for the loss minimization term in (3). Loss minimization is often seen as less important in the introduction and seemingly adds more complexity to the problem, but without it a true optimum may not exist. Even with the additional term, relative "flatness" of the solution space makes finding a unique optimum solution to this problem difficult. Two methods to solve (3) are presented in the next section.

III. Optimal Dispatch Solution Methods

The simultaneous voltage regulation and loss minimization problem (3) can be solved using a heuristic search algorithm with a nonlinear, unbalanced network. Additionally, a linearized, decoupled system of equations can be used in conjunction with classical optimal dispatch techniques.

A. Particle Swarm Optimization (PSO)

Due to the nonlinear nature of (3), as well as the highly unbalanced nature of some distribution networks, such as the one considered in this paper, a closed form analytical solution is extremely difficult to achieve. However, there exist open-source software that can readily solve $\boldsymbol{G}(\boldsymbol{x}, \boldsymbol{u}, \boldsymbol{d}) = \boldsymbol{0}$ for some given $\boldsymbol{u}$ and $\boldsymbol{d}$. Taking advantage of this fact, the OpenDSS [13][14] tool developed by EPRI can be used to set a certain network state, $\boldsymbol{d}$, then attempt to find reactive power injections, $\boldsymbol{u}$, that would result in the network state, $\boldsymbol{x}$, that satisfies (3). As long as the solution space is smooth and continuous, the computational intelligence search method particle swarm optimization (PSO) can be used to find a solution that minimizes the objective function, $\boldsymbol{J(x, u)}$. It works by updating a simultaneous number of solution guesses, called "particles", in directions that have proven to minimize the objective among the entire group [15]. However, PSO suffers from an inability to directly handle inequality constraints. As such, to handle the reactive power constraint of (3), a penalty function is added to the objective function that will increase the further a constraint is violated, as described in in (4)-(5).

$$\min_{\boldsymbol{u}} \tilde{J}(\boldsymbol{x}, \boldsymbol{u}) = J(\boldsymbol{x}, \boldsymbol{u}) + \rho \sum_{k}^{p} \varphi_k(u_k) \tag{4}$$

$$\varphi_j(u_j) = \begin{cases} 0, & |u_j| \le q_j^{g,max}(t) \\ \mu + \dfrac{|u_j|}{q_j^{g,max}(t)}, & otherwise \end{cases} \tag{5}$$

Fortunately, PSO is good at handling non-linear objective functions, so long as ρ in (4) is a relatively significant weight, and (5) is designed to "guide" the particles back to the admissible region. Ultimately, the particles converge to the global minimum if the algorithm is well designed, but the time

PSO takes to converge depends on the solution space. The solution space of (4) is "flat" in that large changes in inputs result in relatively small deviations in the objective function.

B. Linearized Optimal Dispatch

Nonlinear optimal solutions, like PSO, typically suffer from high computation times and may not be scalable to large distribution networks. Therefore, in order to broaden the scope and realism of networks checked, a fast, linearized approach is developed that provides an approximation that will still enable one to draw significant conclusions on a distribution network's PV reactive power capabilities. The power flow equations, $\boldsymbol{G(x,u,d)=0}$, of a radial distribution network may be linearized as such [7]:

$$\begin{aligned} P_{j+1} &= P_j + \Delta p_{j+1} \\ Q_{j+1} &= Q_j + q^c_{j+1} - q^g_{j+1} \\ V_{j+1} &= V_j - r_j P_j - x_j Q_j \end{aligned} \tag{6}$$

Each node of a network is represented by the three equations in (6) and is a function of the previous node in the network. The boundary conditions are that the powers $P_n = Q_n = 0$ for a branch ending at node *n* and that voltage $V_0 = V^*$, under the assumption that the substation bus is already regulated to the nominal voltage. The reactive load is q^c_i and the PV real power output is subtracted from the real load, or $\Delta p_j = p^c_j - p^g_j$. The distribution line resistances and reactances are r_j and x_j. The network is approximated to be *decoupled,* so that (6) in fact represents all three phases of the distribution network as they may be solved simultaneously as individual single phase circuits. Under the classical dispatch problem of power systems, the minimum occurs under the following conditions [16]:

$$\hat{\boldsymbol{J}} = \boldsymbol{J(x,u)} + \boldsymbol{\lambda}^T \boldsymbol{G(x,u,d)} \tag{7}$$

$$\left[\frac{\partial \hat{J}}{\partial \boldsymbol{u}}, \frac{\partial \hat{J}}{\partial \boldsymbol{\lambda}}\right]^T = \boldsymbol{[0,0]^T} \tag{8}$$

The function $\boldsymbol{J(x,u)}$ in (7) is the same objective to be minimized as in (3). Due to the form of (6) and the quadratic nature of $\boldsymbol{J(x,u)}$, the $\boldsymbol{\lambda}$ terms cancel out in (8) and the resulting system of equations is linear. It can then be shown through some derivation that the optimum point that satisfies (8) is achieved by the following matrix form:

$$\begin{bmatrix} \boldsymbol{u} \\ \boldsymbol{P} \\ \boldsymbol{Q} \\ \boldsymbol{V} \end{bmatrix} = \begin{bmatrix} 0 & 0 & \boldsymbol{R} & \boldsymbol{S} \\ 0 & \boldsymbol{I-N} & 0 & 0 \\ \boldsymbol{U} & 0 & \boldsymbol{I-N} & 0 \\ 0 & diag(r_i) & diag(x_i) & \boldsymbol{I-N^T} \end{bmatrix}^{-1} \begin{bmatrix} \boldsymbol{T} \\ \boldsymbol{\Delta p} \\ \boldsymbol{q^c} \\ \boldsymbol{V_n} \end{bmatrix} \tag{9}$$

where $\boldsymbol{N}$ is the connectivity matrix that defines the topology of the network, $\boldsymbol{U}$ is the matrix that defines the PV locations in the network, $\boldsymbol{V_n} = [V^* \; 0 \; 0 \; \cdots 0]^T$ and

$$\boldsymbol{R} = \{[(\boldsymbol{I-N})^{-1}\boldsymbol{U}] \circ [\boldsymbol{r}\boldsymbol{1}^T]\}^T \tag{10}$$

$$\boldsymbol{S} = (path_i \cap path_j) \cdot 2\boldsymbol{x} \tag{11}$$

$$\boldsymbol{T} = \sum_i (path_i \cap path_j) \cdot 2\boldsymbol{x} \tag{12}$$

The operator $\circ$ in (10) is the so-called Hadamard product of matrices, $\boldsymbol{1}$ is a vector of ones, and $\boldsymbol{r}$ is the vector of all line resistances. The sets $path_i$ in (11)-(12) denote all lines that connect from the source node to node *i* and $\boldsymbol{x}$ is the vector of all line reactances. Under this definition, the matrix in (9) is constant for a given network topology and PV placement. Thus, to test many different operating states, $\boldsymbol{d}$, only the right-hand vector needs to be changed. This means that the matrix in (9) only needs to be inverted once and therefore (9)-(12) represents a closed-form analytical solution to the linearized optimal dispatch of $\boldsymbol{u}$.

The inequality constraints of (2) are handled as follows:

1. *Check for violations, if none, then solution is valid*
2. *Set violated PV to* $\hat{q}^g_i = sign\left(q^g_i\right) * q^{g,max}_i$
3. *Set load at violated PV to* $q^c_i - \hat{q}^g_i$
4. *Remove violated PV row and column from (9)*
5. *Solve reduced problem, go to step 1*

IV. Simulation Results

Each solution method is used on the IEEE 13-bus distribution network, which is highly unbalanced. The daily real and reactive loading and insolation profile to be simulated is shown in Fig. 2 along with the resultant PV reactive power capability (shown at 75% penetration).

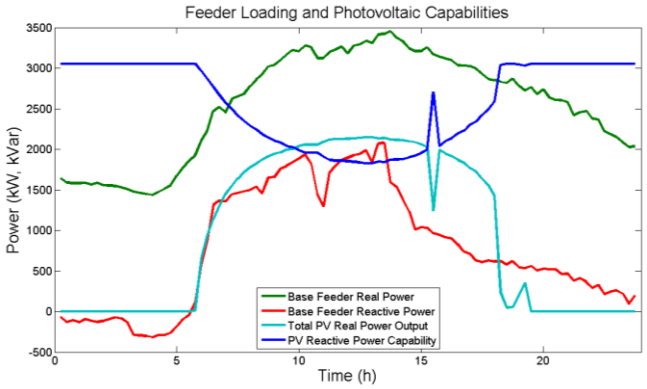

Fig 2. Simulation real (green) and reactive (red) power load and insolation (cyan) and available reactive power at 75% penetration (blue) profiles.

The curves shown in Fig. 2 have been discretized into 15 minute segments, totaling 95 operating states to be tested for each penetration level. Four penetration levels are tested as a percentage of peak load: 25%, 50%, 75%, and 100% for a

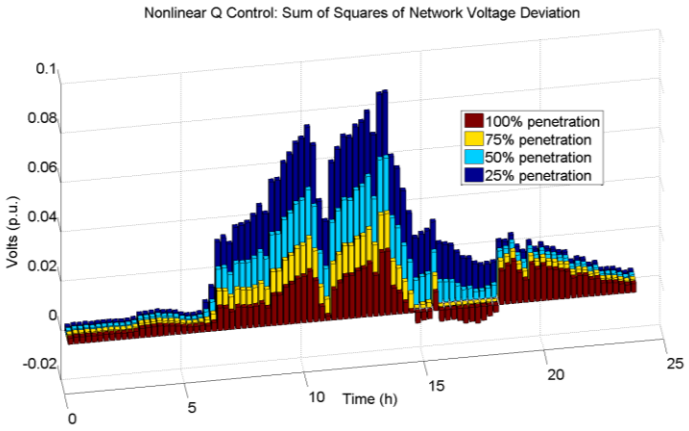

Fig 3. Nonlinear optimization line voltage deviation improvement over no reactive power control case.

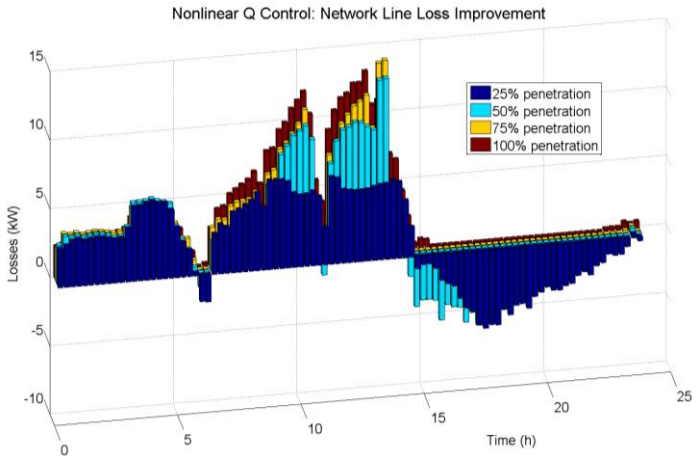

Fig 4. Nonlinear optimization line loss improvement over no reactive power control case.

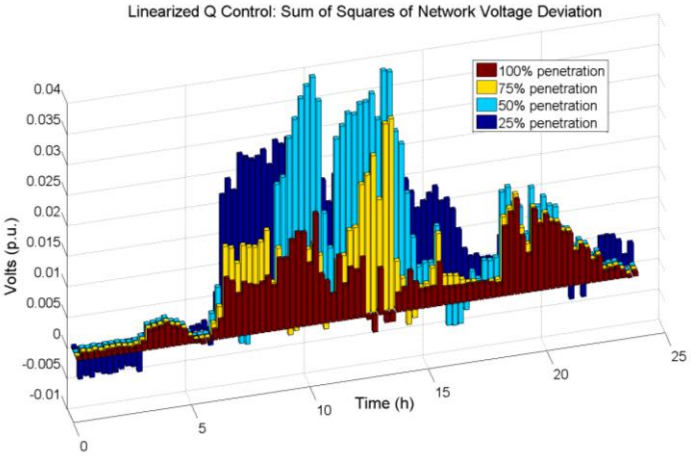

Fig 5. Linearized optimization line voltage deviation improvement over no reactive power control case.

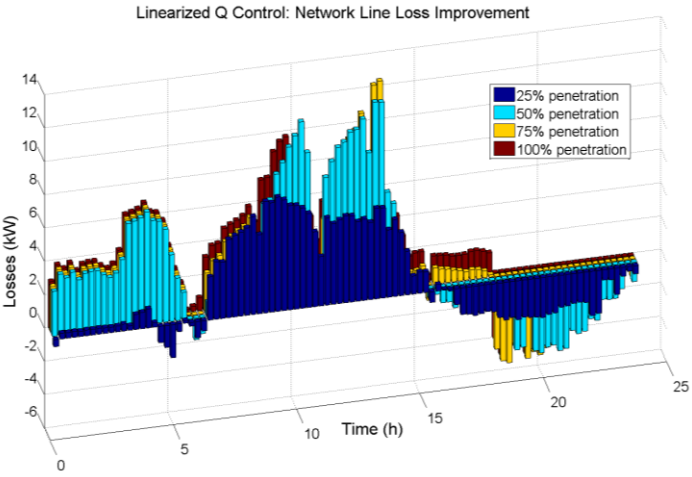

Fig 6. Linearized optimization line loss improvement over no reactive power control case.

total of 380 operating points to be solved. The PV systems are assumed to be uniformly distributed throughout the feeder at each node where a load exists and are sized proportional to the penetration rate and the load to which they are connected. The PSO optimization is run in Matlab in conjunction with OpenDSS via a COM interface. The linearized optimization is run fully in Matlab.

The full nonlinear optimization via PSO took over 100 hours of computation time to solve all 380 operating points and the results are presented in Figs. 3-4. The bar graph in Fig. 3 shows the improved voltage deviation from the base case at each operating point in the day for the four different penetration levels that are tested. The voltage shown is the sum of all the node voltage deviations squared from nominal and then that value is subtracted from the base case sum of voltage deviations where no reactive power control is used, or

$$\delta V^2 = \sum \left(V_i^{base} - V^*\right)^2 - \sum \left(V_i^{Q\ control} - V^*\right)^2 \qquad (13)$$

As such, a more positive value in Fig. 3 indicates a greater improvement over the base case (i.e. there are fewer total voltage deviations). Similarly, Fig. 4 shows the improvement in loss minimization between the full PSO optimized solution and the base case of no reactive power control. Again, a more positive number indicates a greater improvement over the base case. It is clear that there is an overall improvement at each time step for all penetration levels but at times there exists a trade-off between improvement of line losses and voltage profile. This trade-off can be controlled by manipulating the weights w_1, w_2 in (3). Clearly, the most solid improvement that the reactive power control of the PV inverters can achieve is during times of high loading. This seems counter-intuitive since this is also the time at which the PV inverters have the least reactive power capability under "watt priority" control, as most of their ratings are spent outputting real power. Of course the exact extent of the improvement is dependent on the interaction of the PVs with other voltage and reactive

power control equipment, which remained static in these simulations and will require further research. However, the indication here that reactive power control can still play a large role in distribution network power quality management is very encouraging for the future of advanced inverter control schemes in distribution networks. Over all times and penetration levels, the PSO optimization had an average voltage deviation improvement of 0.424V per node, on a 120V scale, and an average line loss improvement of 2.34kW per operating condition.

The linearized optimal solution, in stark contrast to the PSO solution, solved all 380 optimizations in less than one second and its results are presented in the bar graphs in Figs. 5-6. These graphs show the linearized optimal solution for voltage deviation and line loss improvement over the base case, respectively, similar to Figs. 3-4. It is also found that there is a positive improvement at every time and penetration rate in the simulation, although again a trade-off exists between the two minimization goals at times. Overall, the linearized approach is not as successful at achieving the optimization objectives, as is to be expected since it takes advantage of many approximations. The linearized method had a total voltage deviation improvement of 0.338V per node, on a 120V scale, and an average line loss improvement of 1.89kW per operating condition. However, considering the drastic reduction in computational time, these results are very positive as they are relatively close to the nonlinear solution. It is encouraging that this approximation may yield great insights into the reactive power control capabilities of many distribution networks under many PV distributions and operating conditions in future simulations. Perhaps some better approximation of (6) may yield even better results.

Other comparisons worth noting are that between all the results, it is clear that penetration level plays a significant role in control of reactive power and that an increase in penetration has differing impacts on the two minimization goals. That is to say an increase in PV penetration rate seems to result in greater line loss improvement over the base case, although there appear to be diminishing returns. At same time, increasing PV penetration seems to have a negative impact on the voltage deviation improvement. This is perhaps mostly due to the voltage rise effect of the large PV power output that is positively countering the voltage sag of high loading for the larger penetration rates. It just so happens that this is a positive impact for this feeder, as a lightly loaded network would be negatively impacted by the voltage rise and may result in a greater improvement in the voltage profile due to reactive power control as PV penetration increases.

To clarify this observation, the average feeder voltages for each operating condition are plotted in Fig. 7. The voltages for the base case can be seen increasing with PV penetration during the middle of the day while the PVs are outputting real power. This increase counteracts the voltage sag that would otherwise exist with no PV output. However, even though Figs. 3,5 show a diminishing impact of the inverters to regulate voltage as penetration increases, the regulated voltages in Fig. 7 show that this is largely due to there being little need for regulation. Indeed, the linear dispatch nearly

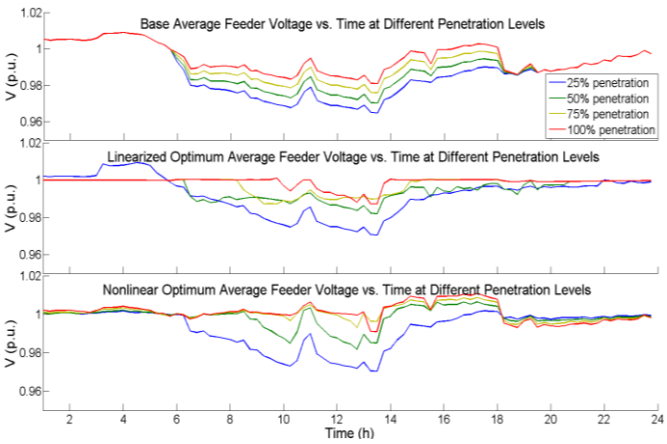

perfectly regulates the voltage for most of the day for a PV penetration greater than 50%.

Lastly, there is consistently a trade-off during nighttime hours in Figs. 3-6 between the two objectives. It would appear that often line losses are incurred to improve the voltage profile. Future research could study the weighting of the minimization goals in terms of what is desirable at a given operating condition. It may be the case that dynamic weights can be given as a function of operating condition.

V. Conclusions

This paper presents the formulation of an optimal reactive power control problem and PSO is presented as well as a linearized approximate solution that requires very little computation time. The two methods are compared and the results of the linearized approach are deemed to yield a good approximation of the capability of PV inverters to regulate voltage and minimize line losses. Having a good approximate solution is important in order to pursue future simulations of large numbers of distribution network topologies, PV placement distributions, and network operating conditions. These future studies will lend better insight into the capabilities of PV inverters to provide voltage regulation and line loss minimization as well as which network conditions are favorable to achieve these goals.

Fig 7. Average feeder voltage at different operating conditions for (top) base case, (middle) linearized optimum, and (bottom) nonlinear optimum.

REFERENCES

[1] "Global market outlook for photovoltaics 2013-2017", May 2013, [Online], Available: http://www.epia.org/.

[2] T. Mason, "San Diego Distributed Solar PV Impact Study",July 2013, [Online], Available: http://www.sandiego.edu/epic/.

[3] R.A. Walling, R. Saint, R. Dugan, J. Burke, and L. Kojovic, "Summary of Distributed Resources Impact on Power Delivery Systems," *IEEE Transactions on Power Delivery*, Vol. 23, No. 3, pp. 1636-1644, July 2008.

[4] J.W. Smith, R. Dugan, and W. Sunderman, "Distribution Modeling and Analysis of High Penetration PV", *Power and Energy Society General Meeting, 2011 IEEE*, pp. 24-29, July 2011.

[5] *IEEE Standard for Interconnecting Distributed Resources with Electric Power Systems*, IEEE Std. 1547-2003, 2003.

[6] E. Troester, "New German grid codes for connecting PV systems to the medium voltage power grid," *2nd International Workshop on Concentrating PV Power Plants: Optical Design, Production and Grid Connection*, Darmstadt, Germany, Mar. 2009.

[7] K. Turitsyn, P. Sulc, S. Backhaus, and M. Chertkov, "Options for Control of Reactive Power by Distributed PV Generators," *Proceedings of the IEEE*, 2011.

[8] M. Fazeli, J. Ekanayake, P. Holland, and P. Igic, "Exploiting PV Inverters to Support Local Voltage - A Small-Signal Model", *IEEE Transactions on Energy Conversion*, Vol. PP, no. 99, pp. 1-10, 2014.

[9] M. J. Reno, R. J. Broderick, and S. Grijalva, "Smart Inverter Capabilities for Mitigating Over-Voltage on Distribution Systems with High Penetrations of PV," *Photovoltaic Specialists Conference (PVSC), 2013 IEEE 39th*, pp. 3153-3158, June 2013.

[10] E. Dall'Anese, S. Dhople, and G. Giannakis, "Optimal Dispatch of PV Inverters in Residential Distribution Systems", *IEEE Transactions on Sustainable Energy*, Vol. PP, No. 99, pp. 1-10, 2014.

[11] H. Xin, Z. Qu, L. Chen, D. Qi, D. Gan, and Z. Lu, "A distributed control for multiple PV generators in distribution networks," *American Control Conference (ACC) 2011*, pp. 1063-1068, July 2011.

[12] H.D. Chiang, M. Baran, "On the Existence and Uniqueness of Load Flow Solution for Radial Distribution Power Networks," *IEEE Transactions on Circuits and Systems*, Vol. 37, No. 3, pp. 410-416, 1990.

[13] R. C. Dugan and T. E. McDermott, "An open source platform for collaborating on smart grid research," *Power and Energy Society General Meeting, 2011 IEEE*, pp. 1,7,24-29, July 2011.

[14] M. J. Reno and K. Coogan, "Grid Integrated Distributed PV (GridPV)," Sandia National Laboratories SAND2013-6733, 2013.

[15] J. Kennedy and R. Eberhart, "Particle swarm optimization," *Proc. IEEE ICNN*, Vol. 4, No. 1, 1989.

[16] A. Bergen and V. Vittal, *Power System Analysis.* New Jersey: Prentice Hall, 2000.

Sandia National Laboratories is a multi-program laboratory managed and operated by Sandia Corporation, a wholly owned subsidiary of Lockheed Martin Corporation, for the U.S. Department of Energy's National Nuclear Security Administration under contract DE-AC04-94AL85000